UCRL-JC-133981
PREPRINT

Room-temperature laser action at 4.3-4.4 μm in $CaGa_2S_4:Dy^{3+}$

M. C. Nostrand
R. H. Page
S. A. Payne
W. F. Krupke
P. G. Schunemann

This paper was prepared for and presented at the
Conference on Lasers and Electro-Optics '99
Baltimore, Maryland
May 23-28, 1999

April 22, 1999

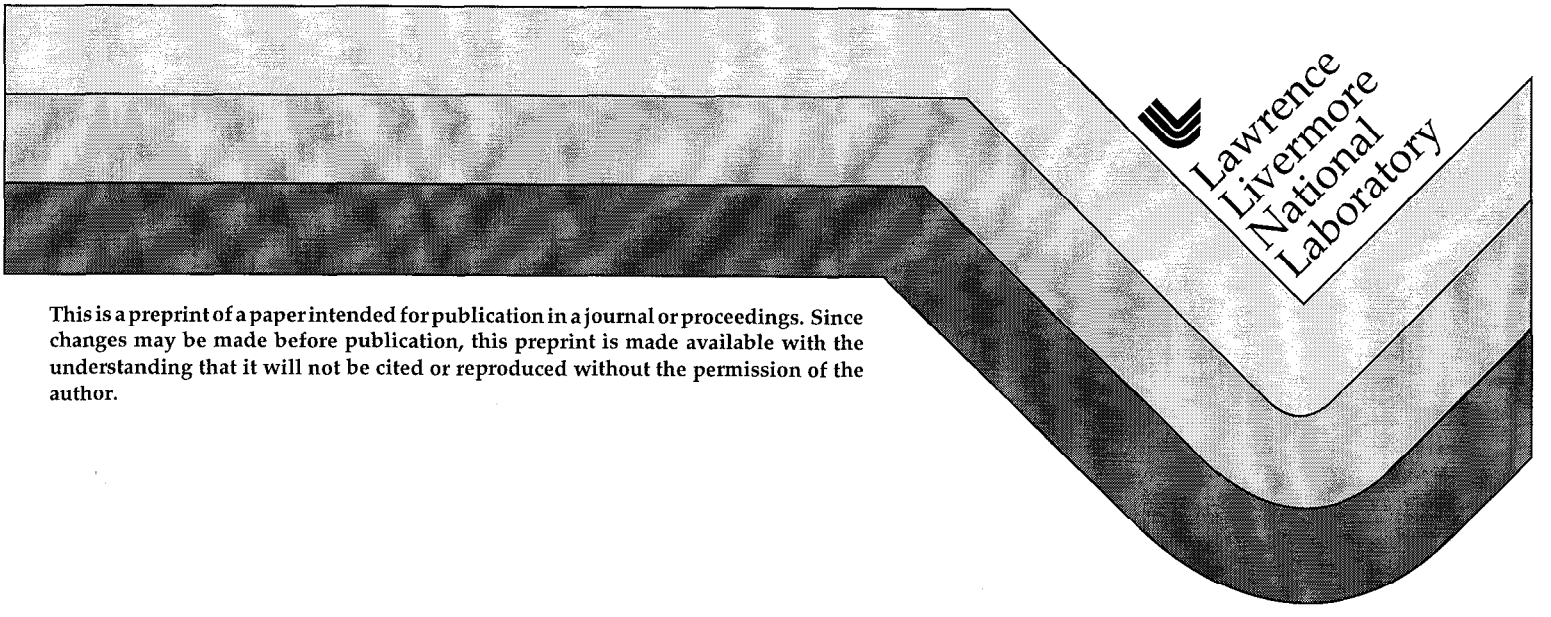

This is a preprint of a paper intended for publication in a journal or proceedings. Since changes may be made before publication, this preprint is made available with the understanding that it will not be cited or reproduced without the permission of the author.

DISCLAIMER

This document was prepared as an account of work sponsored by an agency of the United States Government. Neither the United States Government nor the University of California nor any of their employees, makes any warranty, express or implied, or assumes any legal liability or responsibility for the accuracy, completeness, or usefulness of any information, apparatus, product, or process disclosed, or represents that its use would not infringe privately owned rights. Reference herein to any specific commercial product, process, or service by trade name, trademark, manufacturer, or otherwise, does not necessarily constitute or imply its endorsement, recommendation, or favoring by the United States Government or the University of California. The views and opinions of authors expressed herein do not necessarily state or reflect those of the United States Government or the University of California, and shall not be used for advertising or product endorsement purposes.

Room-temperature laser action at 4.3-4.4 μm in $CaGa_2S_4:Dy^{3+}$

M.C. Nostrand, R.H. Page, S.A. Payne, and W.F. Krupke
University of California, Lawrence Livermore National Laboratory
L-482, Livermore, CA 94550
nostrand1@llnl.gov

P.G. Schunemann
Sanders, A Lockheed Martin Company
P.O. Box 868, Nashua, NH 03061-0868

Abstract: We report room-temperature mid-IR laser operation in a new low-phonon-frequency, non-hygroscopic host crystal $CaGa_2S_4$ (calcium thiogallate). Laser action at 4.31 μm on the $^6H_{11/2} \rightarrow {}^6H_{13/2}$ transition of trivalent dysprosium was achieved with a slope efficiency of 1.6%.

OCIS codes: (140.3380) Laser materials; (140.3580) Lasers, solid-state; (140.5680) Rare-earth and transition metal solid-state lasers

Introduction

Due to applications such as remote-sensing and IR countermeasures, there has been a great deal of interest in solid-state mid-IR (3-10 μm) lasers.[1,2,3,4] Currently, optical parametric oscillator systems (OPO's) are typically used to cover these wavelengths. They incorporate both non-linear media and pump sources, leading to some complexity and sensitivity in the optical system. These issues could be circumvented with direct light generation in solid-state laser media. To avoid luminescence quenching, hosts for these direct lasers must have maximum phonon frequencies below ~350 cm^{-1}, effectively ruling out traditional oxides and fluorides at longer wavelengths. While room-temperature laser operation has been observed previously in some fluoride hosts beyond

4 μm,[5,6] special efforts had to be taken to overcome the extremely low (< 0.01%) radiative quantum yields of these materials. More success has been achieved for laser operation in rare-earth doped oxide and fluoride hosts between 3 and 4 μm (Dy^{3+} [7,8,9], Pr^{3+} [10], Er^{3+} [11,12,13,14] and Ho^{3+} [15,16,17,18].) Sulfide and chloride hosts have received the most attention for laser action beyond 4 μm because of their lower vibrational frequencies. Laser operation beyond 7 μm has been achieved in $LaCl_3$,[19] a low-phonon-energy chloride host that is hygroscopic. Identifying a low-phonon-frequency crystal that incorporates rare-earth ions and resists attack by moisture has been difficult. We report 4.3-4.4 μm lasing on the $^6H_{11/2} \rightarrow {}^6H_{13/2}$ transition of Dy^{3+} in crystalline $CaGa_2S_4$ (see Figure 1), a host that is *not moisture sensitive.* To our knowledge, this is the first report of laser action beyond 4 μm in any rare-earth-doped sulfide. Previous work in $CaGa_2S_4$ was concerned with phosphor studies.[20,21] Spectroscopic data and 1.4 μm laser operation in $CaGa_2S_4$:Dy^{3+} were reported previously by the present authors.[22]

Crystal growth and physical properties

$CaGa_2S_4$ is biaxial, belonging to the orthorhombic crystal class (space group Fddd) and possesses a maximum phonon frequency of ~ 350 cm^{-1}.[23] The 1.5 x 1.2 x 0.7 cm^3 sample used in our experiments was cut from a 19 mm-diameter x 100 mm single crystal grown at Sanders by the horizontal gradient freeze technique in a two-zone transparent furnace.[24,25] Dy^{3+} was doped on the Ca^{2+} site to an estimated concentration of 8 x 10^{19} cm^{-3} (2.0 mol% in the melt and an estimated 60% distribution coefficient). Na^+ was also added (2 mol%) to maintain charge balance. Two axes of the biaxial indicatrix were

identified at extinction positions in a polariscope. These directions have been labeled 'slow' and 'fast'.

Spectroscopy

In our previous work,[22] spectroscopic data relevant to laser operation such as absorption cross sections, emission cross sections (σ_{em}), and lifetimes (τ_{upper}) were measured for a sample of $CaGa_2S_4:Dy^{3+}$. A Judd-Ofelt analysis yielded radiative lifetimes (τ_{rad}), branching ratios (β), and radiative quantum yields ($\eta = \tau_{upper}/\tau_{rad}$). Table 1 gives these data for the present laser sample. The Dy^{3+} energy level diagram indicating the pump and laser transitions is shown in Figure 1. Figure 2 shows the absorption spectrum, polarized along the 'slow' and 'fast' sample axes described above. Notice that the absorption at 1.32 μm (the laser pump wavelength) is almost 5 times greater along the 'fast' axis, making it the preferred pump polarization.

Table 1. Spectroscopic data for $CaGa_2S_4:Dy^{3+}$.

Transition	λ (μm)	τ_{upper} (ms)	τ_{rad} (ms)	η (%)	β (%)	σ_{em} (10^{-20} cm^2)
$^6H_{11/2} \rightarrow {}^6H_{13/2}$	4.3	3.02	4.16	73	7	0.7

Experimental setup

The uncoated rectangular almost-parallelepiped sample was placed in the center of a 20 cm confocal cavity and end-pumped at normal incidence by a Nd:YAG laser operating at 1.319 μm (and 1.338 μm) with 75 μs, 1 Hz pulses. To avoid walk-off along the two polarization axes of the sample and maximize absorption, the input beam was polarized

along the 'fast' axis with a calcite polarizer. The pump spot profile was measured by a razor scan and fit to a Gaussian (1/e amplitude) radial spot size of 350 +/-10 μm. A 1500 nm long-pass filter and 10 cm CaF_2 lens imaged the IR laser light at a 77K InSb detector for temporal waveform acquisition, or to a Molectron J3-09 pyroelectric detector for slope-efficiency measurements. A glass slide pick-off and Molectron J-25 pyroelectric detector measured the input pump energy. The laser output spectra were recorded with a 1-meter, 300 groove/mm grating monochromator located a few meters from the cavity. A calcite polarizer measured the polarization state of the mid-IR output. Although the sample had a 'laser-grade' polish, its end faces were not perfectly parallel. A wedge angle of ~3 mrad was determined by examination of reflections of a single He-Ne laser beam from both end faces of the sample.

4.31 μm laser results

Four cavity mirrors were employed for 4.3 μm operation with transmissions of 0.84% (high reflector or 'HR'), 0.84%, 2.55%, and 7.65% (output coupler or 'OC'). Data was recorded for three mirror configurations with total transmissions (HR + OC) of 1.68%, 3.39%, and 8.49%. Due to strong fundamental CO_2 absorption (~ 0.0025 cm^{-1} at 4.3 μm), the cavity was purged with dry nitrogen for operation near 4.3 μm. Pump energy was limited by concerns of damage, whose threshold was estimated at ~ 15 J/cm^2 of absorbed fluence. Absorbed energy is calculated from incident energy via the relation[26]

$$E_{abs} = E_{inc}\,(1-R_F)(1-e^{-\alpha l})(1-R_F e^{-\alpha l})^{-1} \qquad (1)$$

where E_{inc} is the laser energy incident on the sample, R_F is the Fresnel reflectivity, α is the absorption coefficient at the pump wavelength, and l is the sample length. Threshold estimates were made using a well-known formula for end-pumped lasers[6]

$$E_{abs}^{th} = \frac{\pi(w_p^2 + w_l^2)}{4\sigma_{em}\eta_p} \frac{hc}{\lambda_p} (L+T) \quad (2)$$

where w_p is the minimum pump beam radius in the sample, w_l is the laser waist calculated based on cavity parameters, σ_{em} is the emission cross section, η_p is the pumping efficiency (the fraction of absorbed pump photons that populate the upper laser level), L is the round-trip passive loss in the cavity (to be inferred from a Findlay-Clay plot), T is the total transmission (HR + OC), and λ_p is the pump wavelength. Slope efficiency was calculated using the formula[27]

$$\eta_{slope} = \eta_p \eta_B \frac{\lambda_p}{\lambda_l} \frac{T}{(L+T)} \quad (3)$$

where η_B is the pump and laser beam overlap factor, calculated assuming Gaussian beam profiles, and λ_l is the laser wavelength.

Slope efficiency curves are shown in Figure 3 for two of the cavity configurations, and all data are summarized in Table 2, which includes the predicted result values. A Findlay-Clay plot of absorbed energy threshold vs. total transmission is shown in Figure 4, yielding a passive loss of L = 0.9% +/- 0.3%. This low value is perhaps expected if the

scattering losses obey a Rayleigh λ^{-4} dependence and the Fresnel losses imposed by the ~ 3 mrad sample wedge are compensated by the confocal cavity geometry.

Threshold measurements agreed relatively well with calculated thresholds, but slope efficiency measurements were an order of magnitude below the calculated values. The discrepancy has not been resolved. Notice that the slope efficiencies do not vary greatly with the different output coupler reflectivities, as expected when the passive losses L << T. There may be additional losses not compensated by greater output coupling (such as optical aberrations in the sample). AR-coated samples, and samples with better optical quality, planned for future experiments, may perform better.

Table 2. Summary of $CaGa_2S_4:Dy^{3+}$ 4.31 μm laser threshold and slope data. A passive loss value of L = 0.9 % was used to calculate thresholds and slope efficiencies.

Total output coupling (%)	**Measured threshold (mJ)**	**Calculated threshold (mJ)**	**Measured slope efficiency (%)**	**Calculated slope efficiency (%)**
1.7	1.3	2.1	1.1	12.3
3.4	2.4	3.5	1.6	14.9
8.5	5.2	7.7	1.4	17.0

The laser output and fluorescence emission spectra are shown in Figure 5. The laser output of an unpurged cavity (peak wavelength 4.38 μm) is also shown in this figure for comparison. The extra loss imposed by the CO_2 absorption (~ 5% per pass for T = 1.7%) forced the laser to operate at a longer wavelength. These data suggest tuning is possible in the range 4.25 –4.70 μm. The purged-cavity laser spectrum near 4.31 μm includes the

CO_2 absorption along the ~2 meters of unpurged pathlength between the laser and the monochromator. The laser light was polarized along the 'fast' sample axis.

Conclusions

$CaGa_2S_4$ (calcium thiogallate) has proven to be a viable, non-hygroscopic host material suitable for mid-IR laser operation. We have demonstrated tunable room-temperature laser action around 4.3-4.4 μm in this low-phonon-energy host. This opens the door for compact, direct solid-state lasers operating in the 2-5 μm range important for remote sensing and IR countermeasures.

Acknowledgments

Our gratitude is extended to Peter Thelin, who polished the laser crystal. This work, supported by the Defense Advanced Research Projects Agency and the Department of Energy's Office of Basic Energy Sciences, was performed under the auspices of the U.S. Department of Energy, Lawrence Livermore National Laboratory, Contract No. W-7405-ENG-48.

Figure Captions:

1) Energy levels and laser scheme of trivalent dysprosium.
2) Polarized absorption spectrum for $CaGa_2S_4:Dy^{3+}$, which is biaxial.
3) Slope efficiency curves for $CaGa_2S_4:Dy^{3+}$ at 4.31 μm. T is the total mirror transmission (HR + OC)
4) Findlay-Clay plot of absorbed energy threshold vs. total mirror transmission. A round-trip passive loss of L = 0.9 % is deduced from the data.
5) Emission spectrum and laser output near 4.3 μm in $CaGa_2S_4:Dy^{3+}$. When purged with nitrogen, the laser operates at the peak (4.31 μm) of the fluorescence spectrum. When unpurged, the added loss due to ambient CO_2 absorption forces the laser to operate at a longer wavelength (4.38 μm).

Figure 1

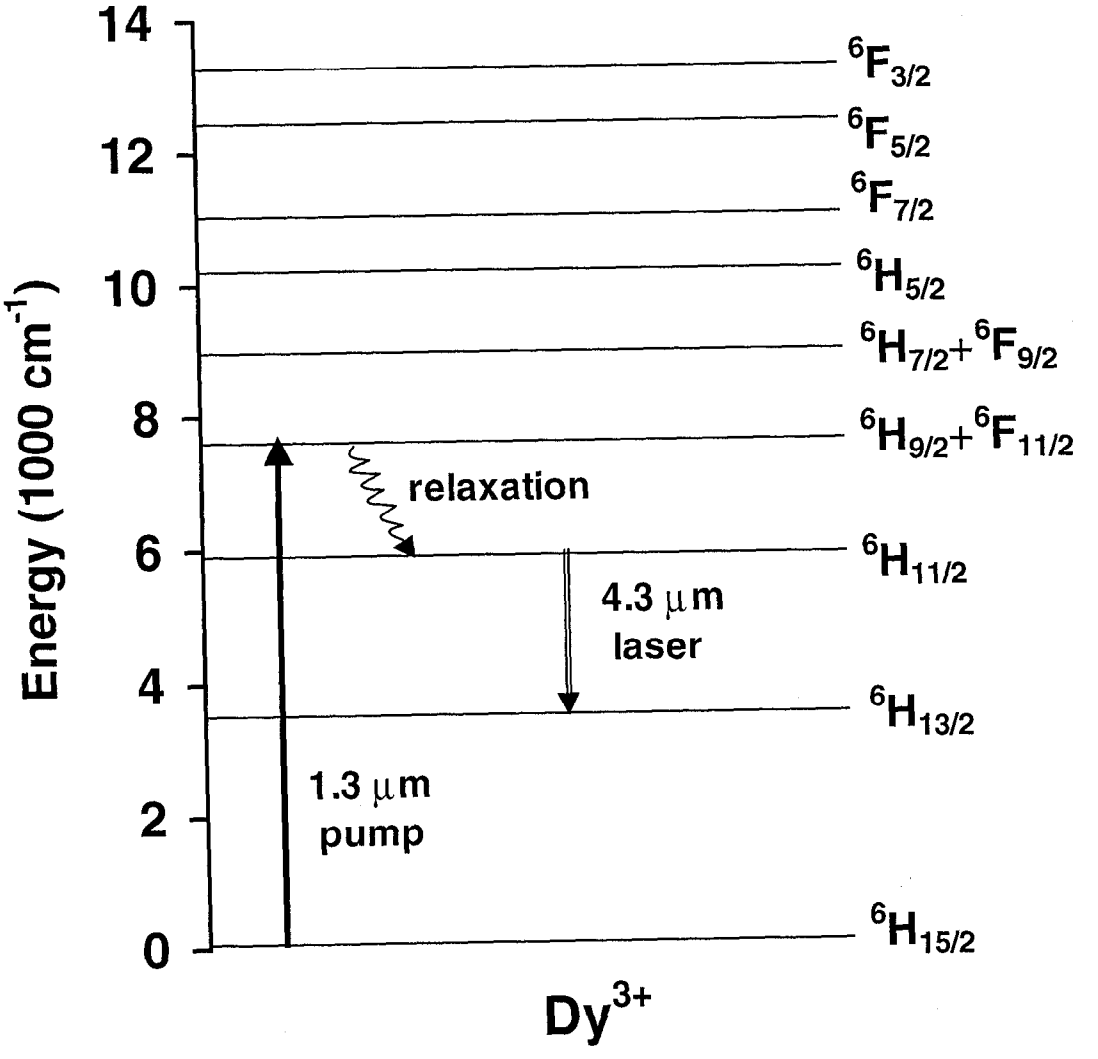
14
12
10
8
6
4
2
0
Energy (1000 cm-1)
6F3/2
6F5/2
6F7/2
6H5/2
6H7/2+6F9/2
6H9/2+6F11/2
relaxation
6H11/2
4.3 μm
laser
6H13/2
1.3 μm
pump
6H15/2
Dy3+

Figure 2

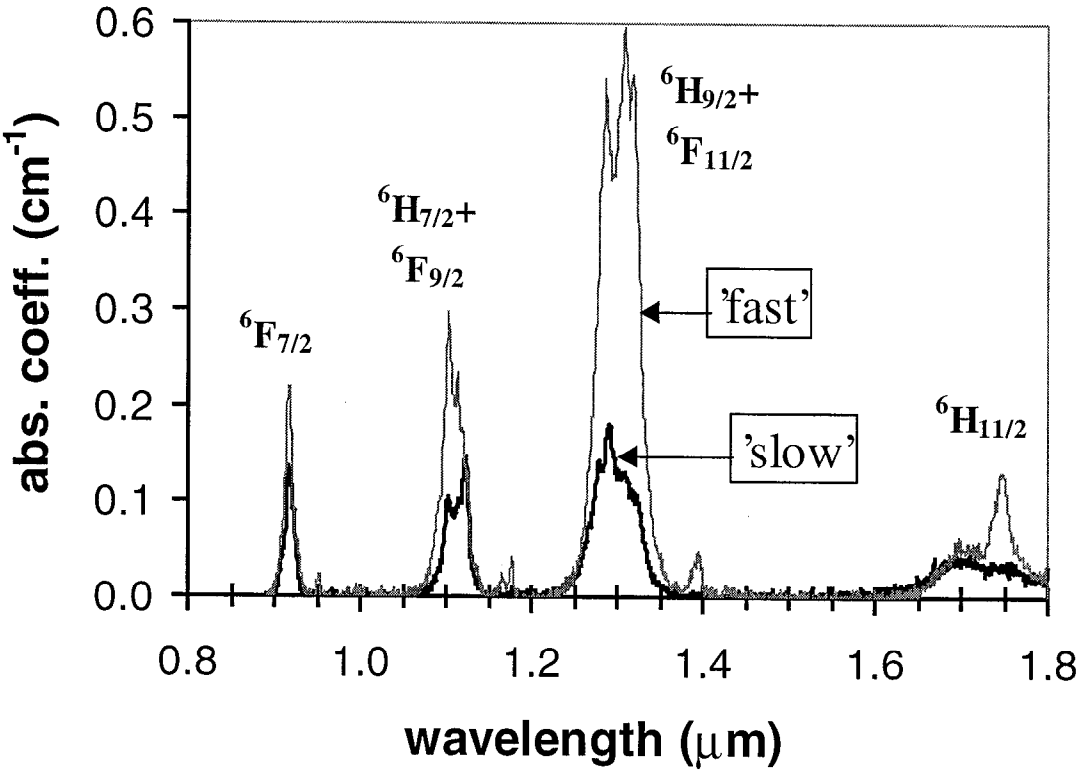
0.6
0.5
0.4
0.3
0.2
0.1
0.0
abs. coeff. (cm-1)
0.8
1.0
1.2
1.4
1.6
1.8
wavelength (μm)
6F7/2
6H7/2+
6F9/2
6H9/2+
6F11/2
6H11/2
'fast'
'slow'

Figure 3

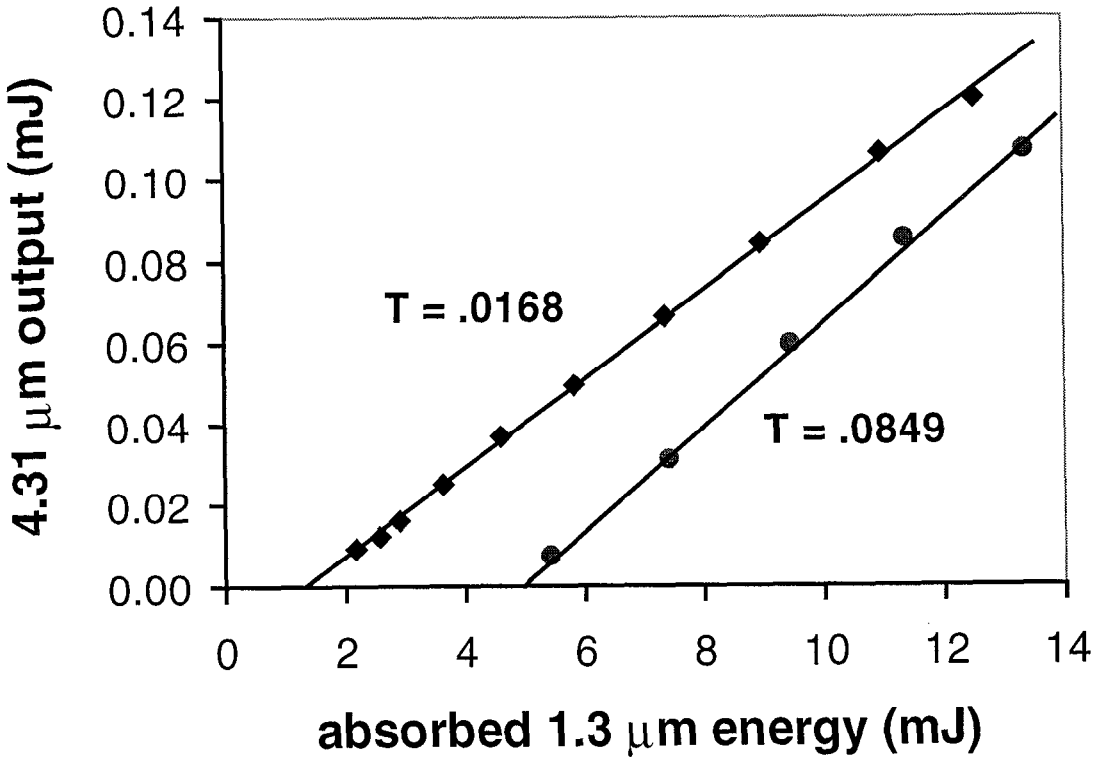
0.14
0.12
0.10
0.08
0.06
0.04
0.02
0.00
4.31 μm output (mJ)
T = .0168
T = .0849
0
2
4
6
8
10
12
14
absorbed 1.3 μm energy (mJ)

Figure 4

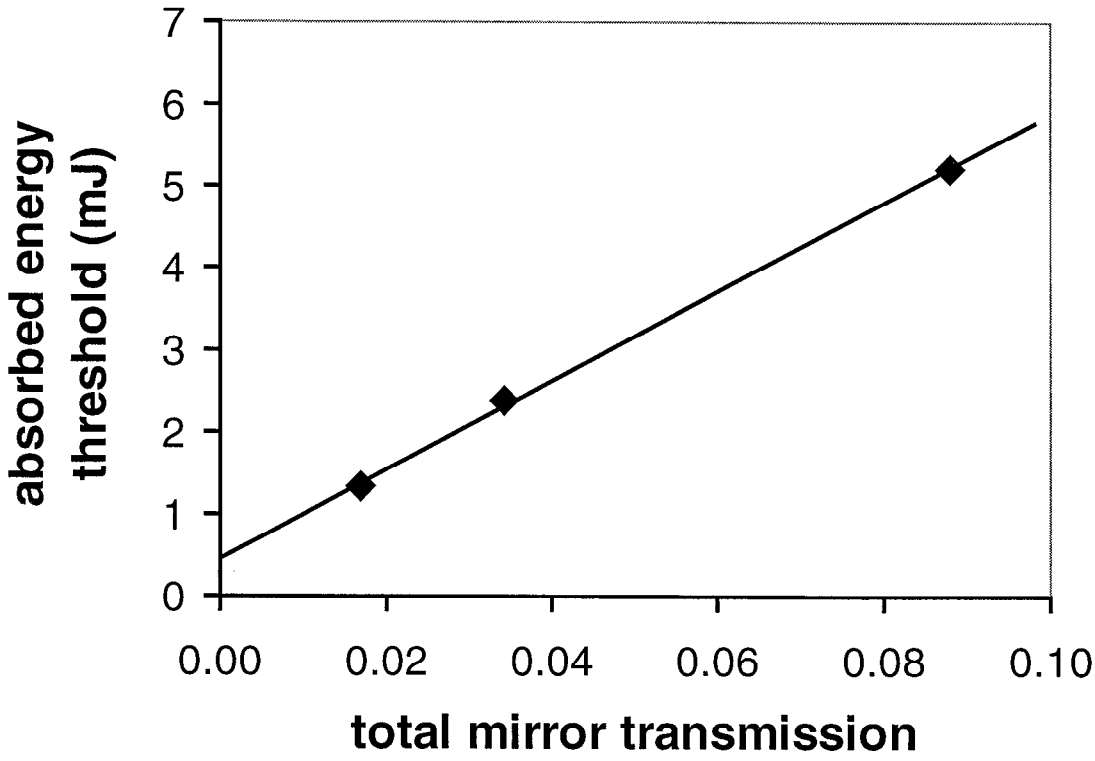
absorbed energy threshold (mJ)
7
6
5
4
3
2
1
0
0.00
0.02
0.04
0.06
0.08
0.10
total mirror transmission

Figure 5

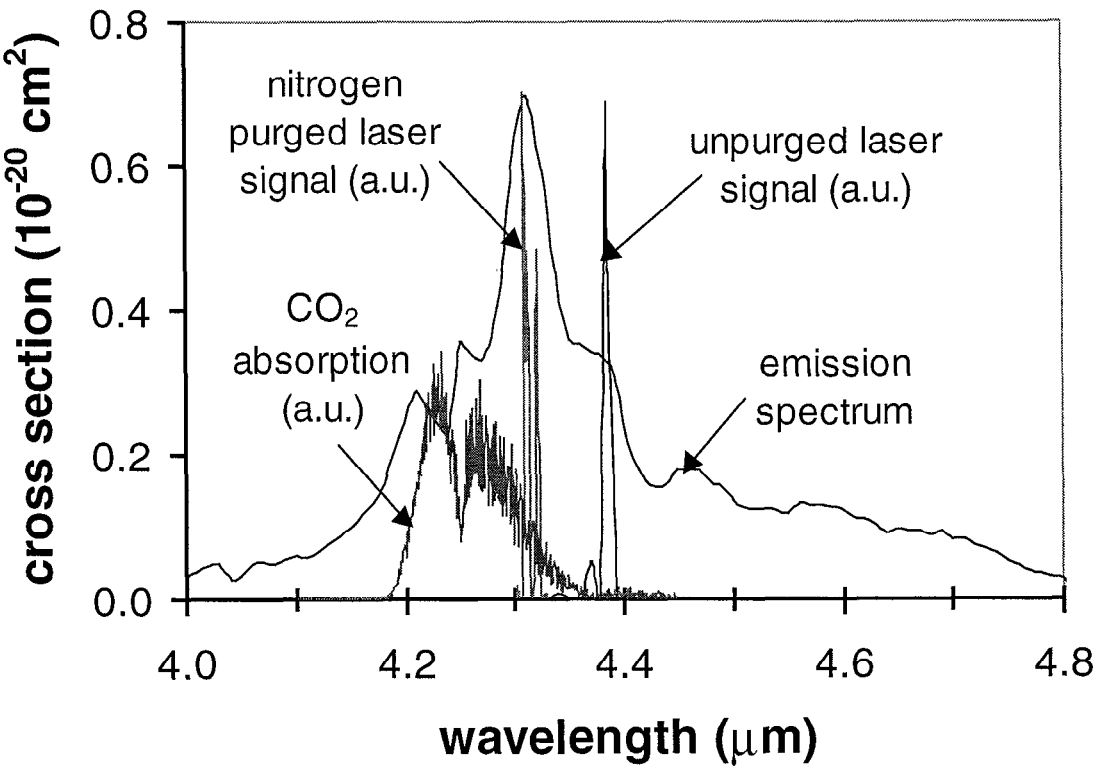
0.8
0.6
0.4
0.2
0.0
cross section (10^{-20} cm^2)
nitrogen purged laser signal (a.u.)
unpurged laser signal (a.u.)
CO_2 absorption (a.u.)
emission spectrum
4.0
4.2
4.4
4.6
4.8
wavelength (μm)

References

[1] S. R. Bowman, L.B. Shaw, S. Searles, S.M. Kirkpatrick, J. Ganem, I. Gambaryan, T. Sanamyan, E. Vartanyan, and B.J. Feldman, *ASSL TOPS* **XIX,** 534 (1998)

[2] T. Schweizer, D.W. Hewak, B.N. Samson, and D.N. Payne, *J. Luminescence* **72**, 419 (1997)

[3] J. Heo and Y. B. Shin, *J. Non-Cryst. Solids* **196**, 162 (1996)

[4] K. Wei, D.P. Machewirth, J. Wenzel, E. Snitzer, and G.H. Sigel, *Opt. Lett.* **19**, 904 (1994)

[5] N.P. Barnes and R.E Allen, *IEEE J. Quantum Electron.* **27**, 277 (1991)

[6] A.A. Kaminskii, in *Proc. Int. Conf. Lasers-80*, Ed. by C.B. Collins (STS Press, McLean, VA 1981), p. 328

[7] L.F. Johnson and J.J. Guggenheim, *Appl. Phys. Lett.* **2**, 96 (1973)

[8] N. Djeu, V.E. Hartwell, A.A. Kaminskii, and A.V. Butashin, *Optics Letters* **22**, 997 (1997)

[9] B.M. Antipenko, A.L. Ashkalunin, A.A. Mak, B.V. Sinitsyn, Yu. V. Tomashevich, and G.S. Shakhkalamyan, *Sov. J. Quantum Electron.* **10**, 560 (1980)

[10] A.A. Kaminskii, K. Kurbanov, and T.V. Uvarova, *Izv. Akad. Nauk SSSR Neorg. Mater.* **23**, 1049 (1987)

[11] J.F. Pinto, G.H. Rosenblatt, and L. Esterowitz, *Electron. Lett.* **30**, 1596 (1994)

[12] A.A. Kaminskii, Izv. *Akad. Nauk SSSR Ser. Fiz.* **45**, 348 (1981)

[13] P.F. Moulton, J.G. Manni, and G.A. Rines, *IEEE J. Quantum Electron.* **24**, 960 (1988)

[14] M.V. Petrov and A.M. Thachuk, *Opt. Spectroscopy* **45**, 81 (1978)

[15] J. Machan, M. Bass, and M. Birnbaum, in *Digest Tech. Pap. CLEO '88* (OSA/IEEE, Washington, D.C., 1988) p. 414

[16] A.A. Kaminskii, T.I. Butaeva, and A.O. Ivanov, *Sov. Tech. Phys. Lett.* **2**, 308 (1976)

[17] R.C. Eckardt, L. Esteorwitz, and I.D. Abella, in *Digest Tech. Pap. CLEO '82* (OSA/IEEE, Washington, D.C., 1982) p.160

[18] L. Esterowitz, R.C. Eckardt, and R.E. Allen, *Appl. Phys. Lett.* **35**, 236 (1979)

[19] S. R. Bowman, L.B. Shaw, B.J. Feldman, and Joseph Ganem, *IEEE J. Quantum Electron.* **32,** 646 (1996)

[20] T.E. Peters and J.A. Baglio, *J. Electrochem. Soc.* **119**, 230 (1972)

[21] A.N. Georgobiani, B.G. Tagiev, O.B. Tagiev, and B.M. Izzatov, *Inorganic Materials* **31**, 16 (1995)

[22] M.C. Nostrand, R.H. Page, S.A. Payne, W.F. Krupke, P.G. Schunemann, and L.I. Isaenko, in *ASSL TOPS* **XIX,** (OSA/IEEE, Washington, D.C., 1998) p. 524

[23] R. Ibanez, A. Garcia, C. Fouassier, and P. Hagenmuller, *J. Solid State Chem.* **53**, 406 (1984)

[24] P.G. Schunemann and T.M. Pollack, U.S. Patent No. 5,611,856 (March 18, 1997)

[25] P.G. Schunemann and T.M. Pollack, *J. Crystal Growth* **174**, 278 (1997)

[26] J.A. Caird, S.A. Payne, P.R. Staver, A.J. Ramponi, LL. Chase and W.F. Krupke, *IEEE J. Quantum Electron.* **24**, 1077 (1988)

[27] W. Koechner, *Solid-State Laser Engineering*. (Springer, New York ,1996) p. 98